NJC

Accepted Manuscript

This is an *Accepted Manuscript*, which has been through the Royal Society of Chemistry peer review process and has been accepted for publication.

Accepted Manuscripts are published online shortly after acceptance, before technical editing, formatting and proof reading. Using this free service, authors can make their results available to the community, in citable form, before we publish the edited article. We will replace this *Accepted Manuscript* with the edited and formatted *Advance Article* as soon as it is available.

You can find more information about *Accepted Manuscripts* in the Information for Authors.

Please note that technical editing may introduce minor changes to the text and/or graphics, which may alter content. The journal's standard Terms & Conditions and the Ethical guidelines still apply. In no event shall the Royal Society of Chemistry be held responsible for any errors or omissions in this *Accepted Manuscript* or any consequences arising from the use of any information it contains.

ROYAL SOCIETY OF CHEMISTRY

www.rsc.org/njc

Revised 09012015- 2015 POM V10 MoV9 Shape Analysis

Submit to New Journal of Chemistry

Size and shape trump charge in interactions of oxovanadates with self-assembled interfaces: Application of Continuous Shape Measure analysis to the decavanadate anion

Irma Sánchez-Lombardo,[1] Bharat Baruah,[1,2] Santiago Alvarez,[3] Katarina R. Werst,[1] Nicole A. Segaline,[1] Nancy E. Levinger[1] and Debbie C. Crans*[1]

[1] Department of Chemistry, Colorado State University, Colorado 80523-1872, USA

[2]Department of Chemistry, Kennesaw University, 370 Paulding Avenue, MD#1203, Kennesaw, GA 30144

[3]Departament de Química Inorganica, Institut de Química Teorica i Computacional (IQTCUB), Universitat de Barcelona, Martí i Franques, 1-11, 08028 Barcelona, Spain.

Abstract:

Polyoxometalates can serve as versatile catalysts in aqueous media. Solvation of these compounds is critical to their catalytic properties. In the studies reported here, we employ ^{51}V NMR spectroscopy, dynamic light scattering and continuous shape analysis to probe the solvation of two polyoxometalates, decavanadate and monomolybdononavanadate, encapsulated in reverse micelles. The ^{51}V NMR chemical shift reports on the protonation state of the oxometalate while its linewidth reveals the local environment sensed by the oxometalate in the reverse micelle. We have shown that placement of decavanadate in several protonation states in a microemulsion results in spectroscopic observation of the deprotonated $[V_{10}O_{28}]^{6-}$ (V_{10}) molecule (Baruah et al. *J. Am. Chem. Soc.,* **2006** *128* (39):12758-65). Previous studies have shown that the oxometalate requires at least 2-3 layers of water to stabilize it in the reverse micelles and present work shows that no differences are observed whether oxometalate has a charge of -5 or -

6. The dynamic light scattering studies demonstrate that the size of the reverse micelles containing polyoxometalate does not change significantly upon loading. Finally, continuous shape measure (CShM) further describes the structural perturbation of V_{10} as one of the V-atoms is replaced with a heteroatom. CShM analysis shows minor structural perturbation of the oxovanadate core with heteroatom replacements even though the charge and thus overall polarity of the anion changes. Similarly, the continuous shape measure analysis of protonated forms of V_{10} show that the variation related to protonation of the V_{10} anion does not significantly change the shapes of the different classes of vanadium atoms within the compact oxoanion even though the charge and thus overall polarity of the anion changes. Thus, the change in shape and steric interactions are very minor because any change in geometry is counteracted by changes elsewhere in the structure. This study represents the first application of shape measures to oxometalates. Because size and shape could both be critical for interaction with interfaces, two differently charged oxometalates are placed in a nanosized water droplet to investigate how they are solvated. Because little change was observed in the ^{51}VNMR spectra and smaller changes were found in the size, we conclude that the shape was most important for this interaction and that changes in charge appeared to have a smaller impact on the system.

corresponding author: email Debbie.Crans@ColoState.edu

20 words for TOC text

Using ^{51}V NMR spectroscopy, dynamic light scattering and continuous shape analysis to characterize two polyoxometalate-encapsulation in reverse micelles.

I. Introduction

Polyoxometalates (POMs) are large inorganic anionic species with many useful properties in synthesis, catalysis and biology.[1-9] POMs are generally compact large structures, and they have a wide range of shapes resulting in many different materials. Some fundamental classes of POMs such as Keggin and Dawson anions are important building blocks with similar shapes; however, replacing individual atoms in these POMs causes local distortions and result in molecules with similar shapes but with different symmetry that influence their overall properties such as charge and polarity. For example, POMs are versatile catalysts for many reactions in water and other media however the specific composition determines their properties as catalysts.[10-12] The interaction of polyoxometalates with the environment solvating them critically influences their catalytic properties.[13-15] Here, we explore the impact of decavanadate (Fig. 1a), a class of polyoxometalates and modified decavanadate (Fig. 1b-1c) in a confined nanosized water droplet.

Reverse micelles (RMs) are generally very flexible and dynamic nanoscale droplets of water sequestered near a layer of a surfactant such as sodium bis(2-ethylhexyl)sulfosuccinate (AOT, Fig. 1d), which separates the aqueous phase from a bulk nonpolar liquid phase.[16, 17] When solvated in nanosized aqueous pools, polyoxometalates in RMs will interact with the solvating water and affect the properties of this water dramatically presumably because of their high charge. Many different experiments and simulations have probed the micellar environment, and much is known about the water molecules inside the RM and their different behavior comparing it to in bulk solution.[18-38] For example, hydrogen bonding interactions between water molecules differs for water at the surfactant interface from water from at the core, bulk-like water in the RMs.[39] How molecules such as the large polyoxometalates are encapsuled in RMs

is of general interest because of the applications of RMs systems for templating-synthesis of nanoparticles.

In this work we measure the spectroscopic signatures of two simple POMs, decavanadate (V_{10}) and monomolybdononavanadate (V_9Mo) (see Fig. 1) when confined in nanosized water droplets defined in RM structures. We expect that the confinement of POMs will be different if charges and sizes of the POM varies, and that such difference can be measured., Observable differences may be particularly likely if the POM interacts with water sequestered near the surfactant layer of the aqueous phase and distinct from a bulk aqueous phase in the interior of the RM. We have determined that the presence of these two different polyoxoanions, decavanadate (V_{10}) and a molybdenum-containing V_{10} (V_9Mo) using dynamic light scattering to measure RM size. In addition, we evaluated potential changes by ^{51}V NMR spectroscopy and in the structure of the oxometalates using the continuous shape measure (CShM) analysis. However, as described below because of the stringent requirements of the quality of the X-ray structures used in CShM analysis, the only substituted decavanadate currently suitable for this analysis is the structure shown in Fig. 1c (see discussion below). Together, the experimental studies with these complex anions of -5 and -6 charge in RMs are compared with the CShM analysis to examine the importance of charge and size, respectively, by confinement in a nanoscale space.

Recently, we have reported on studies using vanadium oxometalates to probe the interior of RMs.[40-42] The substantial charge found on the oxometalates leads them to solubilize in the RM interior. In the work reported here, we have used two different decametalates, decavanadate in two different protonation states, ($[HV_{10}O_{28}]^{5-}$ and $[V_{10}O_{28}]^{6-}$ abbreviated HV_{10} and V_{10}), and monomolybdononavanadate, $[V_9MoO_{28}]^{5-}$ (abbreviated V_9Mo) [43], whose structures are shown in Fig. 1. V_{10} is thermodynamically stable in aqueous solutions from pH 3 to 6 [44] and although not

the thermodynamically preferred form, can persist above pH 6 for a few days because the kinetics of its hydrolysis to form other vanadate oligomers is so slow.[45] Three geometrically different vanadium atoms comprise each V_{10} molecule: two equatorial V_A, four equatorial V_B and four axial V_C. Each vanadium atom is bound to six oxygen atoms in a slightly distorted octahedral environment (Fig. 1a). Protonation of the V_{10} change the overall charge and polarity of the anion. Although the bridging oxygen atoms are most basic the protons are not likely to remain in one location and as such the protonation will change the polarity of the anions. V_9Mo [43] presents an analog of V_{10} in which one V_C is replaced with a Mo atom, as depicted in Fig. 1b. The overall charge on this polyanion is -5. Although reasonably large, the decametalate dimensions (shown in Fig. 1) allow them to sit comfortably in the interior of mid-sized RMs, $w_0 \geq 6$ (where $w_0 = [H_2O]/[\text{surfactant}]$ [17]). Studies with the structurally related POM anion allowed further exploration that the results obtained with the V_{10} anion and it is likely that both structure and charge of the anion are important.

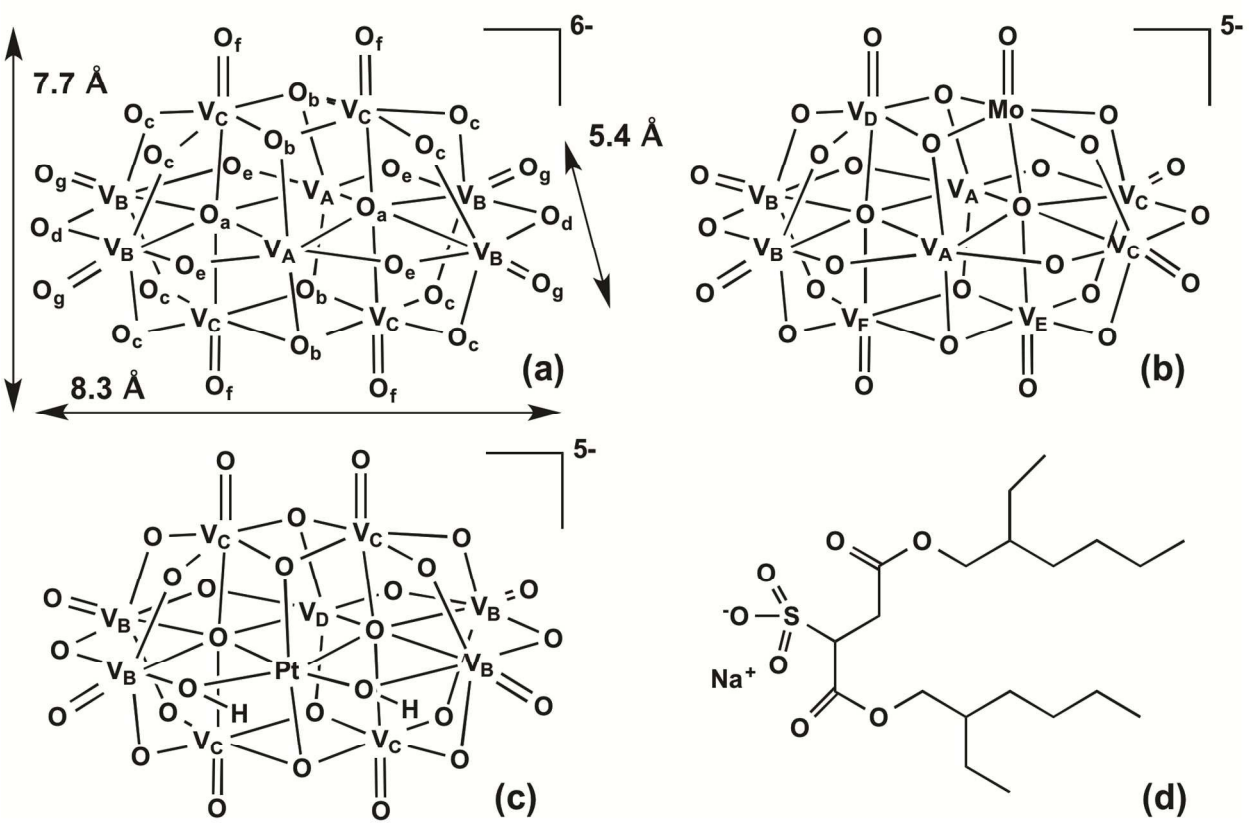

Fig. 1. Structures of (a) $[V_{10}O_{28}]^{6-}$ (V_{10}), (b) $[V_9MoO_{28}]^{5-}$ (V_9Mo) (c) $[H_2PtV_9O_{28}]^{5-}$ and (d) AOT.

The CShM analysis allows us to focus on the molecular shape and evaluate distortions in the bioctahedral V_{10} / V_9Mo core as well as in the coordination polyhedron surrounding each specific metal atom within the polyoxometalate. This analysis is based on the comparison between the deformed anion and the pure decavanadate anion and allows us to compare the distortion of different molecules from the same ideal shape on the same scale, as well as distortions of the same molecule from different reference geometries.[46] Specifically, the CShM analysis calculates a distance in 3N-6-dimensional space between the structure to be analyzed and a reference shape, that is independent of size and orientation.[47] We use the method to examine distortions in a regular VO_6 octahedron (OC-6) as well as the edge-sharing V_{10} bioctahedron (eshbOC-10). The resulting shape measures, abbreviated S(OC-6) and S(eshbOC-

10), respectively provide us with simple ways to distinguish different types of distortion. A measure of the distortion of an MO_6 octahedron, however, describes the degree of distortion but not the distortion mode. Differentiating distortion modes can be done by examining the deviation from another ideal structure, such as the trigonal prism (TPR-6) in the case of octahedral six-coordinated metal ions. Because X-ray crystallographic data of sufficient high resolution does not exist for the MoV_9 anion, we carried out the analysis on the only mono-substituted V_{10} suitable for the CShM analysis, a Pt-substituted V_{10} shown in Fig. 1c.

In the work reported here, we present results from experiments probing V_{10} and V_9Mo encapsulated in the aqueous pools of sodium bis(2-ethylhexyl)sulfosuccinate (AOT) RMs and the effects that these provides additional exploration into the results obtained with the V_{10} anion, in particular, related to structure or charge of the anion. The AOT RMs used in this study are formed in isooctane by self-assembly; we vary the size of the water pool by changing w_0.[48] Using ^{51}V NMR, we follow chemical shifts and line broadening for the two poly oxometalates placed in the RMs. We compare the experimental results for these POMs with predictions from CShM to understand RM size measurements. Using the combined approach we are able to probe if the structural and charge perturbation affects the solvation of the POM in the RMs.

II. Experimental Methods

*II. A. Materials***.** Sodium metavanadate, $NaVO_3$ (99.9%), AOT (sodium bis(2-ethylhexyl)sulfosuccinate or docusate sodium salt) (99%) were purchased from Sigma-Aldrich. Sodium molybdate dihydrate, $Na_2MoO_4 \bullet 2H_2O$ (99.9%) was purchased from Strem Chemicals and used as received. AOT was purified by dissolving in methanol and stirring overnight in the presence of activated charcoal.[49] Then filtration and removal of methanol by distillation under

vacuum follows resulting in AOT suitable for use. Doubly distilled deionized water with a specific resistivity of > 18 MΩcm (Barnstead E-pure system) was used throughout this work.

*II. B. Decavanadate and Monomolybdononavanadate solution preparation***.** A series of decavanadate, $V_{10}O_{28}^{6-}$ (V_{10}) stock solutions were prepared at 24.4, 16.3 and 6.5 and 0.7 mM concentration in order to be able to prepare solutions with 0.7 mM V_{10} at different w0 sizes. First $NaVO_3$ was dissolved in doubly distilled deionized water to about 90% of the desired volume in a volumetric flask and then the pH was adjusted to 3 using 6 M HCl resulting in V_{10}. Finally, the pH was raised back to the desired pH (5.0) using 1 M NaOH and doubly distilled deionized water was added to reach the final volume. We prepared samples with these concentrations to enable preparation of RM samples containing the V_{10} with overall V_{10} concentrations of 0.7 mM and spectra are shown in Fig. 2.

Similar to the V_{10} solutions, a series of monomolybdononavanadate, $V_9MoO_{28}^{5-}$ (V_9Mo) stock solutions were prepared following published methods [43] at 32.5, 16.3, 9.75, 6.5 and 0.7 mM concentrations. We dissolve $NaVO_3$ and $Na_2MoO_4.2H_2O$ in a 9:1 ratio in doubly distilled deionized water in a volumetric flask, adjust the pH to 5.0 using 6 M HCl and then add doubly distilled deionized water to generate the required volume. This preparation results in solutions containing primarily V_9Mo with some V_{10} and insignificant amounts of V_xMo_y, where $x<9$, $y>1$, and $x+y=10$. The spectra shown in Fig. 3 have the contribution of V_{10} subtracted in the spectra. That is the signals from V_A, V_B and V_C were subtracted according to the ratio 1:2:2. Specifically, the V_C signal resolved from the other signals in V_9Mo would be integrated and compared to the resolved signals from the V_9Mo cluster (V_A, V_B, V_C or V_F) to determine the ratio of the V_{10} and the V_9Mo species, respectively. The calculation of the samples showed that the V10 to V9Mo ratio for the aqueous solution was 44%. This changed in the RMs samples

with 28% for w_0 = 30, 24% for w_0 = 20, and 27% for w_0 = 12 (for w_0 = 6 the resolution is to poor for accurate determination of the oxometalate).

All RMs solutions were prepared within an hour prior spectral analysis. The pH values of the aqueous solutions were measured before and after measurement at 25°C using a calibrated Orion 420A pH meter. The pH values were adjusted to within 0.05 and pH variability between samples was within 0.1 pH unit unless otherwise noted.

*II. C. AOT Reverse Micelle Preparation***.** A 0.2 M AOT stock solution was prepared at ambient temperatures by dissolving AOT in isooctane. The V_{10} and V_9Mo stock solutions described above were used to make AOT RMs by pipetting stock solutions of aqueous V_{10} or V_9Mo into the AOT stock solution. All samples were mixed by vortexing 2-3 min and then submitted for ^{51}V NMR spectroscopic analysis. The resulting solutions were clear indicating microemulsions formation and yellow because of the presence of the decametalates. The overall concentration of POM in the RMs was 0.7 mM. For V_{10} containing RMs, we prepared w_0 = 8, 12, and 20. This protocol yields RMs with fewer than one V_{10} per RM for w_0 = 8 and 12; for w_0 = 20 there are 1.1 V_{10} per RM, as shown in Table 1. These numbers were calculated using published values for the aggregation number of AOT molecules (n_{agg}) that assemble to form the RMs,[39] the AOT concentration and the POM. The numbers of POM molecules were obtained by dividing the overall POM concentration by the number of RMs in solution, which can be obtained from the AOT concentration and the n_{agg} for a particular size of RMs. For V_9Mo containing RMs, we prepared w_0 = 6, 12, 20 and 30 in which the overall V_9Mo concentration was 0. 7 mM, with an overall V-atom concentration of 6.3 mM.[43] The V_{10} (w_0 values of 8, 12 and 20) or V_9Mo loaded RMs (w_0 = 6, 12, 20, and 30) were prepared

II.D Reverse Micelle Characterization. Experiments were carried out to assure that RMs form in solution using dynamic light scattering (DLS) and conductivity. DLS experiments measured RM size and polydispersity (Wyatt DynaPro Titan) of samples containing 0.1 M AOT.[50] Prior to data acquisition, samples were equilibrated in the DLS instrument for 10 min at 25 °C. Each measurement consisted of a minimum of 12 runs each, each of which is a set number of scans. Scans were performed in a rate of 10 acquisitions for 100 s. The DLS instrument generated correlation functions from scattering of particles in solution. On the basis of our exponential fits to the data, we obtain RMs size with a 10% instrument error. The reproducibilities of the experiments are reported with standard deviation. Sizes measured of the RMs without any probe using DLS were similar to those reported in the literature.[39, 51-54]

RM samples were also characterized by their conductivity using a conductivity meter (Orion 150A) equipped with a glass cell with two rectangular Pt electrodes (15 mm x 10 mm) with cell constant 0.1. The conductivity cell was calibrated with a standard 100 μS/cm solution.

II. E. ^{51}V NMR Spectroscopy of AOT RMs samples. ^{51}V NMR spectra were recorded using both a Varian INOVA-300 MHz and INOVA-500 MHz spectrometer at 78.9 MHz and 131.5 MHz, respectively. Spectra were acquired using routine parameters such as a 83.6 kHz spectral window, a 60˚ pulse angle, and a 0.096 s acquisition time with no relaxation delay for the 300 MHz. For the 500 MHz spectrometer, the spectra were acquired with no relaxation delay using a 39.2 kHz spectral window, a 60˚ pulse angle, and a 0.2 s acquisition time. ^{51}V chemical shifts were referenced against an external sample of VO_4^{3-}, which had been referenced against a sample of $VOCl_3$.[55, 56] For spectral work-up, a 15 Hz exponential line broadening was applied before Fourier transformation. Longitudinal relaxation time (T_1) measurements were performed using the inversion-recovery method and for these studies a spectral width of 6 kHz and tau

values up to 2.7 s were used. The T_1 times were at the mS time-scale as reported previously.[56] The relative intensities and integration of the vanadium signals could therefore be used to calculate the concentrations of V_{10}, V_9Mo and potential other oligomeric species.[56]

II. F. Spectral Analysis and Curve Fitting of RM Spectra. The NMR FIDs collected were Fourier transformed and subjected to phase correction (MestReC V. 4.5.9.1 NMR data processing software for Windows). Resulting spectral peaks were fitted to determine peak heights, shifts and linewidths (OriginPro 7.0 and IgorPro, version 4.01).[41] The samples were referenced against a sample of $VOCl_3$ (0 ppm) using aqueous vanadate in alkaline solution (pH 12) as reported previously.[41] As V_{10} and V_9Mo species are inseparable in solution the ^{51}V NMR signals overlap with each other. A spectrum reflecting V_9Mo alone can be achieved by subtracting the spectrum of 100 % V_{10} at pH 5.0 from the spectrum of 90% vanadium and 10 % Mo at pH 5.0 at 294 K.[43]

II. G. Continuous Shape Measure Analysis. The continuous shape measure analysis of a specific structure *X* is performed in comparison relative to an ideal shape of object *A*. First, we identify a molecule with the ideal shape *A* as the structure that is closest to structure *X*. This search requires optimization with respect to size, orientation in space and pairing of vertices of the two structures as described by Avnir and coworkers. [46, 47, 57] Using this reference shape, we calculate the distances between the equivalent atomic sites from the position vectors $\vec{x}_k$ and $\vec{a}_k$ of the reference and target molecule, respectively, and then calculate the shape measure according to equation 1. Importantly, the denominator in equation 1 is a normalization factor that makes the continuous shape measures (CShM) size independent. By definition, $S_X(A)$ must be minimized with respect to size, orientation and vertex pairing.

$$S_X(A) = \min\left[\frac{\sum_{k=1}^{N}\left|\vec{x}_k - \vec{a}_k\right|^2}{\sum_{k=1}^{N}\vec{a}_k^2}\right]100 \qquad (1)$$

All shape parameters have been calculated with the SHAPE 2.1 program [58], which can be obtained from the authors upon request.[58] To disregard the deviations from ideal geometries due to important bond distance distortions associated to the coexistence of V-O single and V=O double bonds, we have used normalized versions of the X-ray coordination polyhedral throughout. The calculation therefore indicates only the angular distortions, as discussed elsewhere.[46] We retrieved the structural data for V_{10} and V_9Mo that we analyzed from the Cambridge Structural Database (CSD), version 5.36 [59] and from the Karlsruhe Inorganic Crystal Structure Database (ICSD).[60]

III. Results and Discussion

The study presented here uses three different methods to explore how the environment inside RMs affects the POMs encapsulated therein. Through DLS measurements, we observe the size characteristics for POM containing RMs. Comparisons between different POMs informs us about the interactions that dominate the size of the RMs. ^{51}V NMR spectroscopy informs us about the state of the POM inside the RMs. Finally, shape analysis points to similarities and differences between the POM structure, and ties the DLS and ^{51}V NMR data leading to a comprehensive picture of the POMs in the RMs.

III. A. ^{51}V NMR Measures of V_{10} and V_9Mo in Aqueous Stock Solution and in AOT RMs.

Fig. 2 shows ^{51}V NMR spectra collected for V_{10} in aqueous stock solution at pH 5.0 and in the series of RM solutions with w_0 = 8, 12, and 20, prepared as described in sections *II.B and II.C*. We have shown the utility of ^{51}V NMR spectroscopy for characterizing the interior of RMs in previous studies.[40, 61, 62] Similar to our previous reports, the spectra in Fig. 2 show that the V_{10} signals peak at different chemical shifts when they are in the RM compared to bulk aqueous solution.[40] As the RM water pool grows with increasing w_0 value, we observe slight shifting of the V_{10} peaks downfield toward the peak positions for the V_{10} in bulk aqueous solution. We have previously noted that even though other measures of water in AOT RMs indicate that most of the water in a w_0=20 RM behaves like bulk water,[63] the environment sensed by the V_{10} cluster differs significantly from bulk aqueous solution; the V_{10} NMR peaks never come close to the chemical shifts observed for V_{10} in bulk aqueous solution at pH 5.0.

The ^{51}V NMR spectra are consistent with deprotonation of the HV_{10} species that dominates at pH 5 to form V_{10}, the -6 species. This is readily understood considering that V_{10} is involved in the following proton equilibria shown in equations (2) – (4). However, this deprotonation although consistent with previous studies countered our attempt to study both the HV_{10} and the V_9Mo whose charge are identical and gave us a system in which the charge differs by -1.

$$V_{10}O_{28}^{6-} + H^+ \rightleftharpoons HV_{10}O_{28}^{5-} \qquad pK_1 = 5.5\text{-}6.0\ ^{44} \qquad (2)$$

$$HV_{10}O_{28}^{5-} + H^+ \rightleftharpoons H_2V_{10}O_{28}^{4-} \qquad pK_2 = 3.1\text{-}3.7\ ^{44} \qquad (3)$$

$$H_2V_{10}O_{28}^{4-} + H^+ \rightleftharpoons H_3V_{10}O_{28}^{3-} \qquad pK_3 \sim 2.0\ ^{44} \qquad (4)$$

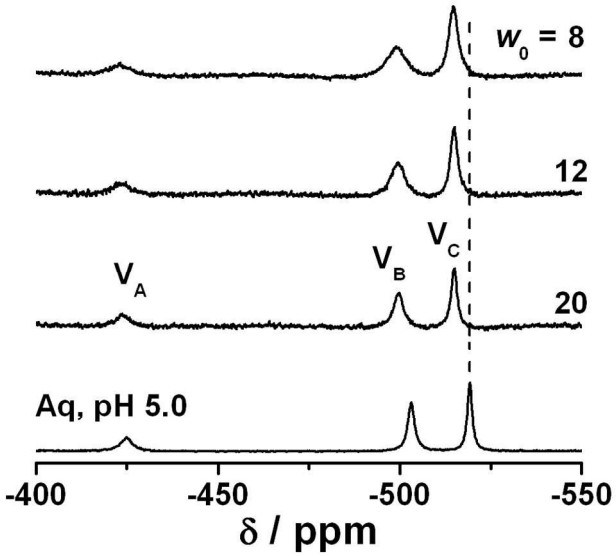

Fig. 2. Representative ^{51}V NMR spectra of V_{10} aqueous stock solution (0.7 mM at pH 5.0), and in AOT reverse micelles with w_0 = 8, 12 and 20 prepared with pH 5.0 solutions of V_{10}. Vertical dashed line indicates the position of the V_C peak in aqueous solution and is included as a guide to the eye (see Fig. 1 for key to V_A, V_B and V_C).

In addition to changes in chemical shifts, the ^{51}V NMR spectral linewidths for V_{10} in RMs are also broader than for V_{10} in aqueous stock solution. The spectra in Fig. 2 show that the linewidths increase with decreasing RM size suggesting an increasingly confined environment as the RM water pool size decreases. Overall, the spectra observed for V_{10} inside the RMs demonstrate differences in the environment compared to those in aqueous solution consistent with our previous reports.[40, 61, 62]

To test whether V_{10} represents an isolated case of an anionic POM in confined environment, we investigated V_9Mo in the same RM environments. The V_9Mo analog of V_{10}, where one of the V_{10} axial vanadium atoms (V_C) has been replaced by a Mo atom, (Fig. 1b) is stable at pH 5.0.[43] V_9Mo has a similar structure and the same charge as the monoprotonated

form of V_{10}, that is, $HV_{10}O_{28}^{5-}$ versus $V_9MoO_{28}^{5-}$. The major difference between V_{10} and V_9Mo is the asymmetry Mo induces when it replaces one of the V_C atoms of V_{10}.

Fig. 3 shows the ^{51}V NMR spectra of aqueous stock solution at pH 5.0 and the series RM solutions containing V_9Mo. Six separate ^{51}V NMR signals appear for V_9Mo in a 2:2:2:1:1:1 ratio [43] in contrast to the three signals in 1:2:2 ratio observed for V_{10}. The presence of V_{10} in the solutions with V_9Mo is evident in the resulting NMR spectra by observation of the additional peaks attributable to V_{10}. To simplify the analysis of changes in V_9Mo signals as the RM environment changes, we show spectra in which we have subtracted the V_{10} signal allowing us to focus on the signals from the V_9Mo. The V_9Mo cluster is an analog of V_{10} (Fig. 3), but the single Mo substitution breaks the symmetry seen in V_{10} leading to six separate ^{51}V NMR signals in contrast to three for V_{10}. As described in the experimental the signals from V_{10} is subtracted by using the integration of the V_C signal from V_{10} that does not significantly overlap with any signals from V_9Mo. For bulk aqueous solution at pH 5.0, the V_{10} signal represents 44% of the complexes in solution. In the RM solutions, we observe different amounts of V_{10} depending on the size of the RM. The following amounts of V_{10} was subtracted from each of the samples shown in Fig. 3; 28% for w_0 = 30, 24% for w_0 = 20, 27% for w_0 = 12 and 41% for w_0 = 6 of the oxometalate. The more complex ^{51}V NMR spectrum for V_9Mo provides us an opportunity to probe the environment around the V-atoms and potentially providing more information as we vary the RM sizes.

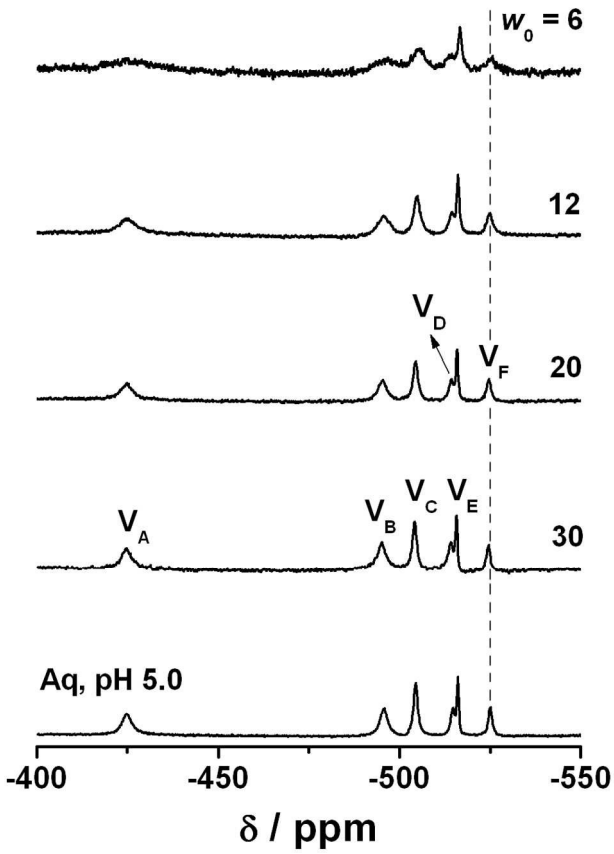

Fig. 3. Representative ^{51}V NMR spectra of V_9Mo aqueous stock solution (0.7 mM at pH 5.0; 7.0 mM metal ions), w_0 = 6, 12, 20 and 30. Spectra have had the pure V_{10} contribution subtracted (28% for w_0 = 30, 24% for w_0 = 20, 27% for w_0 = 12 and 41% for w_0 = 6 of the oxometalate). The vertical dashed line indicates the position of the V_F peak in aqueous solution and is included as a guide to the eye (see Fig. 1 for key to V_A, V_B, V_C, V_D, V_E, and V_F).

The method used to prepare V_9Mo [43] arises from an equilibrium between the V_9Mo isomer shown in Fig. 1b and V_{10}. Because the V_9Mo complexes are somewhat labile, it is noteworthy that we observe signals for V_9Mo even in the smallest RMs where the average number of V atoms per RM is two, far less than the nine or ten that comprise the POM clusters. This demonstrates that the V_9Mo complexes remain intact inside the RMs even for the smallest

RMs (w_0 = 6) investigated, documenting that the V_9Mo is stable even in this environment. Because the V_9Mo and V_{10} are equilibrating, the change in the V_{10}-V_9Mo ratio reflects subtle changes in the environment of the RMs nanosized water droplet. Although the change in the V_{10}-V_9Mo ratio is a modest 6% from w_0 = 30 to w_0 = 20 the change is more dramatic from w_0 = 12 to w_0 = 6 where the increase of 14% corresponding to a 50% increase in V_{10} contribution. The latter change in V10V_9Mo ratio is significant and point to V_{10} being more stable than V_9Mo in the smaller RMs despite its higher charge.

Similar to results for V_{10}, the linewidths for V_9Mo ^{51}V NMR spectra shown in Fig. 3 gradually increase as the RMs shrink from w_0=30 to w_0=6. In RMs with w_0=30, the linewidth values approach those of the bulk solution, which suggests that the water pool is large enough for the V_9Mo molecule to tumble as if it were in bulk water. The significant increase in linewidth for V_9Mo in w_0=6 RMs indicates that the environment confines the V_9Mo molecules enough so that their motion is restricted. We observe different linewidth increases for specific peaks. For example, the V_A peak broadens significantly as observed for the V_{10} cluster. For the signals for V_B and V_C more linebroadening is observed compared to signals V_D, V_E and V_F as the w_0 size of the RMs approach w_0=6. The broadening for V_B and V_C is consistent with hindered motion around several molecular axes as anticipated when the V_9Mo molecule is rotating but is encountering resistance due to a lack of space in the RM water pool. In contrast, the V_E and V_F peaks remain almost the same width in bulk solution and w_0=6. These differences indicate that the RM introduces an increasingly constricted environment that precludes regular motion by these large POMs on the wide axis but not on the smaller axis.

Studies have shown that some fraction of the intramicellar water interacts strongly with surfactant headgroups at the interface.[64] For RMs with w_0 > 10 encapsulating only water, more

than half of the water forms a core away from the interface.[64] The pH = 5.0 value of the aqueous vanadate stock solution introduces the V_{10} and V_9Mo into the solution as highly charged anions. This should result in significant Coulomb repulsion between the AOT headgroups and the oxometalate probe molecules. The dramatic linebroadening of these signals suggests that the oxometalate resides at the intramicellar interface. We have previously observed immobilization of the negatively charged V_{10} molecule in RMs created with a cationic surfactant, CTAB/1-pentanol reverse micelle regardless of the RM size, most likely from strong Coulomb attraction of V_{10} with the positively charged interface.[61] The narrow linewidths observed for spectral signals of V_{10} and V_9Mo when $w_0 > 10$ indicate that these POM molecules stay away from the interface, residing in the "bulk" intramicellar water pool.[40] In the larger RMs, such as $w_0 = 20$, the internal diameter is ~70 Å.[64] Excluding a shell of 5 Å from both sides leaves ~ 60 Å inside the RM.[64] In this environment the V_{10} and V_9Mo can tumble almost as freely as they can in bulk water. Thus, for $w_0 = 20$, the linewidths for V_{10} signals are comparable to aqueous bulk solution, see Fig. 2.

One additional observation adds to our understanding of how the RM affects the solubilized POMs, that is, there is a lower limit to the size RM that can encapsulate a POM. Previously, we have observed that below w_0=6 we cannot stabilize RM solutions containing V_{10}.[62] We observe the same limit for V_9Mo in AOT RMs. This suggests that RMs smaller than w_0=6 are too small to stabilize V_{10} or V_9Mo in their interiors. We explain this on the basis of hydration of both the AOT surfactant headgroups and hydration of the POMs. We have previously observed that the smallest AOT RMs we could prepare that encapsulate V_{10} was w_0=6.[62] For this size RM, there is sufficient water to form a water layer at the AOT surface and a layer at the POM surface. At lower values of w_0, there is not enough water to both hydrate the AOT

headgroup and POM simultaneously. In w_0=6 RMs, all the water present interacts strongly with either the inner surface of the RM or the surface of the POM. This interfacial water has been observed to relax more slowly than bulk water [38, 39] and can lead to the broadening we observe for the ^{51}V NMR spectra of both V_{10} and V_9Mo (Figs. 2 and 3).[65, 66]

Although the linewidths observed for ^{51}V NMR spectra of V_9Mo and V_{10} in RMs follow similar trends, their chemical shifts do not. RM encapsulated V_9Mo shows virtually no change in chemical shift from the peak positions in bulk aqueous solution, regardless of w_0 value. We have attributed the chemical shift changes for V_{10} encapsulated in the RMs due to deprotonation of the V_{10} species.[40] thus producing the POM with a -6 charge in place of the -5 charge for the V_9Mo Replacement of one V atom with a Mo in the V_{10} molecule leads to a oxometalate that is much more acidic with a pK_a of 2.77 compared to the 5.5 for V_{10}, see equation (3) an (5):

$$V_9MoO_{28}^{5-} + H^+ \rightleftharpoons HV_9MoO_{28}^{4-} \qquad pK_a = 2.77\ ^{43} \qquad (5)$$

As a result, for all practical purposes, the V_9Mo solutions created at pH 5.0 for these studies have only one V_9Mo species in solution and that is $V_9MoO_{28}^{5-}$. The dynamic equilibrium between V_{10} and V_9Mo in solution leads the ^{51}V NMR spectra of V_9Mo solutions also to include some V_{10} (subtracted from spectra shown in Fig. 3). The V_{10} signals appearing in V_9Mo solutions display the same shifts associated we observe for pure unprotonated V_{10} in the RMs reported here and previously.[40] The absence of chemical shift changes for V_9Mo in RMs confirms the interpretation that chemical shifts seen for V_{10} arise from variations in protonation equilibrium and are not due to other effects arising from the confined RM environment.

We observe similar linebroadening for both V_{10} and V_9Mo in the AOT RM environment despite the higher charge on V_{10}. The trends in the linewidth thus appear the same regardless of the net charge on the POMs.

III. B. DLS Measurements of POMs in AOT RMs. Table 1 lists hydrodynamic radii of AOT/isooctane RMs containing only water, aqueous V_{10} solution and the aqueous solution containing the V_{10} / V_9Mo mixture as well as the polydispersity of those measurements. DLS polydispersity is a measure of how uniform the particles are. We also include size data from the literature for comparison in Table 1. Our results for AOT/isooctane RMs with only water (no POM) agree very well with previously reported measures.[61, 62] The AOT/isooctane RMs containing V_{10} were similar in size to experiments we have previously reported and, within the uncertainty of the measurements, were no different than the RMs containing only water.[61, 62]

The AOT/isooctane RMs containing the V_{10}/V_9Mo solution will contain either a V_{10} or a V_9Mo or if they are sufficiently large one of each. We calculate that RMs with $w_0 \leq 12$ contain fewer than one POM per RM; larger RMs contain, on average, about one POM per RM. Thus, DLS measurements of these solutions of RMs will, include three different types of interiors: pure water, water and V_{10}, or water and the V_9Mo/V_{10} mixture. Our results for RMs containing either water or water and V_{10} yield essentially the same size. If the V_9Mo leads to RMs with a significantly different size, then we would expect - at a minimum - to see larger polydispersity, and if the effect is large, potentially different hydrodynamic radii. The charge on the V_{10} inside the RM is -6 while the V_9Mo carries a charge of -5. If the overall POM charge affects the packing of the RMs and thus the size of the RM, then we might expect to see a difference in size. The data presented in Table 1 show that, within our ability to measure the size found for the combined V_9Mo/V_{10} mixture was experimentally indistinguishable from that observed for V_{10} and RMs containing only water. Importantly similar behavior is observed between V_{10} and V_9Mo in the AOT RMs' even through they carry different in charge. This suggests that the similarity in shape and size is probably more important for determining the nature of the RMs.

Table 1. The sizes of 0.1M AOT/isooctane RMs that contain water, V_{10} and V_9Mo as determined by DLS. Radii for reverse micelles in nm[a].

w_0	H_2O[b]	H_2O	V_{10}	V_9Mo
6	2.8	3.1 (0.2)	3.6 (0.2) 3.6 (0.2)[c]	3.8 (0.2)
8	3.2	3.40 (0.2)	3.7 (0.3)	4.5 (0.1)
10	3.4		4.4 (0.2)[c]	
12	3.7	3.80 (0.2)	4.6 (0.1)	4.9 (0.1)
20	4.4	4.45 (0.1)	5.0 (0.4)	5.0 (0.3)

[a]The number in parenthesis is the standard deviation for 15-30 acquisitions. [b]Ref 61. [c]Ref 67.

III. C. Continuous shape measures (CShM) analysis of the V_{10} and modified V_{10}. The CShM analysis allows us to explore the how the POM geometry changes upon substitution of one V atom in the V_{10} cluster. Coupling the information on structural changes with ^{51}V NMR studies in RMs describing the environment of two POMs combined with DLS studies determining the size of the RMs containing POMs lead to information on the environments in the RMs. Specifically, we can compare the effect of size (similar for both PMs) and charge (one POM is -4 and the other -5/-6). To carry out a CShM analysis between two similar species requires structural knowledge usually obtained from x-ray diffraction measurements. Although excellent x-ray crystal structures exist for V_{10}, x-ray crystal structures that have been solved for the V_9Mo show significant disorder attributed to the variation in the Mo occupancy.[68]

Unfortunately, this limits the utility of CShM applied to V_9Mo and V_{10}. Because, the V_9Mo x-ray structures are unsuitable for CShM analysis to explore the effect of the Mo heteroatom on the V_{10} geometry we explored the possibility of using alternative V_9M derivatives where M would be a different metal ion.

A number x-ray structures exist for POMs in which one V-atom has been replaced with an alternative atom. [69, 70], $HTeV_9O_{28}^{4-}$ [71], $H_2TeV_9O_{28}^{3-}$ [72], $HIV_9O_{28}^{3-}$ and $IV_9O_{28}^{4-}$ [73]. We searched the crystal structure database (CSD) to identify other monosubstituted POMs that could serve as a good proxy for the V_9Mo complexes and provide atomic coordinates for comparison. Several potential structures emerged from this search including $H_2PtV_9O_{28}^{5-}$ [69, 70], $HTeV_9O_{28}^{4-}$ [71], $H_2TeV_9O_{28}^{3-}$ [72], $HIV_9O_{28}^{3-}$ and $IV_9O_{28}^{4-}$ [73]. Because of the stringent and precise atomic location requirement needed for CShM analysis, the only the x-ray structure with sufficiently high resolution to carry out the CShM analysis was $H_2PtV_9O_{28}^{5-}$ (PtV_9).[69] Because this structure was doubly protonated, it was important that we also explore the impact of protonation equilibria on the structure of the decametalates.

Before performing the CShM analysis on the monosubstituted V_{10}, we first analyzed the shapes of the homometallic V_{10} atoms found in the CSD. We chose a ten vertex edge-sharing bioctahedron (eshbOC-10) formed by two fused regular octahedral, shown in Scheme 1, as a reference shape against which we compared the metal core of the V_{10} anions found in the CSD.

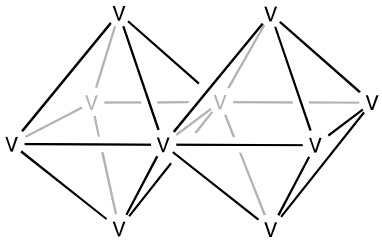

eshbOC-10

Subsequently we characterize the coordination polyhedra of the V-atoms with a threefold purpose: (a) To characterize the distortions of the three types VO_6 octahedra (V_A, V_B and V_C in Fig. 1); (b) to verify if different degrees and patterns of protonation have structural influence on those octahedra; and (c) to study the effect of metal substitution on the shape of the MO_6 octahedra (M = V, Pt).

The CShM analysis first focused on 74 unprotonated decavanadate structures [74-135] yielded rather small shape measures relative to the reference geometry, with an average S(eshbOC-10) = 0.05(2) and a maximum value of 0.14. Single protonation of decavanadate does not significantly alter the geometry of the metal skeletons; their shape measures relative to the eshbOC-10 are on average 0.05(1). However this value is based on only five structures. Higher degrees of protonation, in $H_nV_{10}O_{28}^{-(6-n)}$, have only a minor effect on the geometry of the V_{10} core, with average S(eshbOC-10) values of 0.10(4), 0.11(2), 0.09(3) for n = 2, 3 and 4, respectively. If the 83 structures including all degrees of protonation are considered together [102, 103, 136-184], the average measure is S(eshbOC-10) = 0.10(3), indicative of only minor structural variability. We have also considered the possibility of structural influence by hydrogen bonding between decavanadate and the cations, but neither the shortest hydrogen-bonded distance nor the number of hydrogen bonds seem to correlate with the small changes observed in the bioctahedral shape measures.

Replacing a vanadium atom in the V_{10} complex by Pt to generate the PtV_9 anion does not affect the overall shape of the metal core. The CShM value is 0.03. We therefore established that the shape of the decametallate core is quite robust and suffers little distortions from ideality, regardless of the nature of the metal ions.

After establishing that the shape of the decametalate core suffers little distortions from ideality, we turn our attention to the individual positions of the oxygen atoms that constitute the outer envelope of the polyoxometalate. To that end we have carried out a shape analysis of the coordination polyhedra of the three types of vanadium atoms, first for the unprotonated anions and then for the protonated ones, to ascertain any stereochemical effects associated to protonation. Two types of terminal unbridged oxo ligands (O_f and O_g illustrated in Table 2) have V=O double bond character. The CShM analysis reveals significant distortion of the coordination sphere due to bond distance differences. To minimize effects of bond distance distortions, we configured the analysis by distance-normalizing the coordination polyhedra so that the resulting shape measures are sensitive only to angular distortions. In addition, we have repeated the analyses with the experimental coordination bond distances distortions to make sure that our conclusions are not biased by the use of normalized distances.

We first present analysis of the bare, unprotonated, V_{10} anion structures calculating the shape measures of the VO_6 groups for the three types of vanadium atoms, V_A, V_B and V_C, relative to the octahedron and the trigonal prism. These shape measures are plotted in a shape map (Fig. 4a). Although these structures are far from the Bailar interconversion pathway between the octahedron and the trigonal prism, the TPR-6 shape measure allows us to discriminate the different distortions undergone by the V_B and V_C atoms. In that map the V_A, V_B and V_C atoms occupy each well defined regions. The V_A atoms, that have only single V-O bonds, appear closer to the ideal octahedron than V_B and V_C, each having a V=O double bond.

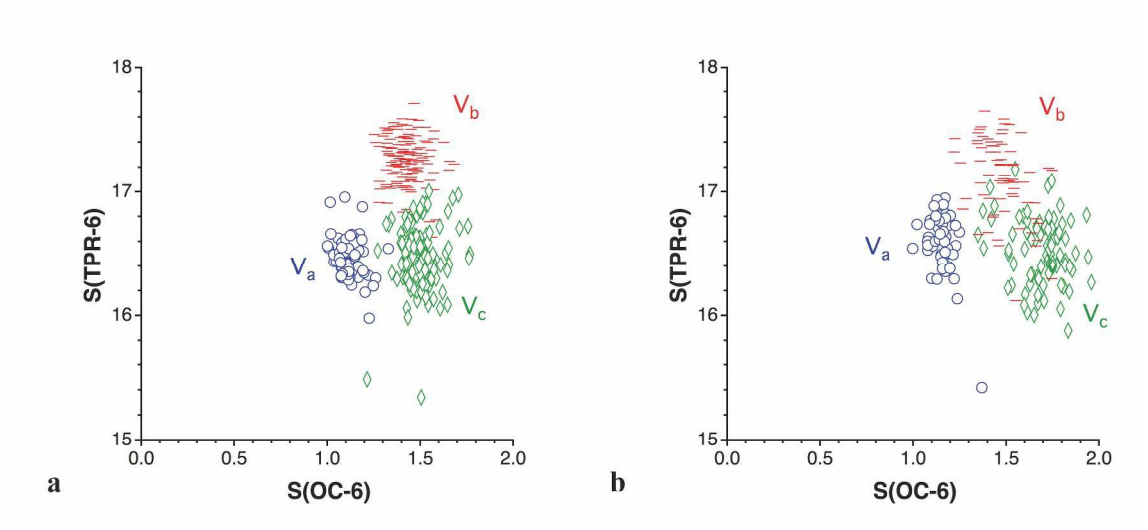

Fig. 4. Position of the normalized polyhedra of the three types of VO_6 groups in (a) unprotonated and (b) protonated decavanadates on a shape map relative to the regular octahedron (OC-6) and the trigonal prism (TPR-6).

We have also analyzed the structures of V_{10} anions crystallized with several degrees of protonation, including the unprotonated $V_{10}O_{28}^{6-}$ form, as well as the structures of $HV_{10}O_{28}^{5-}$, $H_2V_{10}O_{28}^{4-}$, $H_3V_{10}O_{28}^{3-}$, and $H_4V_{10}O_{28}^{2-}$. We also considered $H_5V_{10}O_{28}^{-}$ and the neutral $H_6V_{10}O_{28}$ even though we could not locate crystal structures for them and their protonation positions are either unassigned or assigned arbitrarily. All the $VO_{6-n}(OH)_n$ polyhedra in the protonated anions, regardless of their degree of protonation (Fig. 4b), occupy the same regions of the shape map. We observed insignificant dispersion for V_A and V_C. However, as anticipated, some dispersion was observed for V_B because the oxygen atoms associated with these sites correspond to protonation sites. It was surprising that such a modest dispersion was calculated for the corresponding shape measures.

Table 2. Protonated oxygen sites and affected vanadium coordination spheres for different degrees of protonation (n) of decavanadates. Key for the oxygen atoms are shown in Fig. 1a.

n	Site	Modified coordination spheres

1	O_c	$V_BO_5(O_cH)$, $V_CO_5(O_cH)$
2	O_b, O_b	$V_AO_5(O_bH)$, $V_CO_5(O_bH)$
	O_b, O_c	$V_AO_5(O_bH)$, $V_BO_5(O_cH)$, $V_CO_4(O_bH)(O_cH)$
	O_c, O_c	$V_BO_5(O_cH)$, $V_CO_5(O_cH)$
	O_f, O_f	$V_CO_5(O_fH)$
3	O_b, O_c, O_c	$V_AO_5(O_bH)$, $V_BO_5(O_cH)$, $V_CO_4(O_bH)(O_cH)$
	O_c, O_c, O_e	$V_AO_5(O_eH)$, $V_BO_5(O_cH)$, $V_BO_4(O_cH)(O_eH)$, $V_BO_5(O_cH)$
4	O_b, O_b, O_b, O_b	$V_AO_4(O_bH)_2$, $V_CO_4(O_bH)_2$
	O_b, O_b, O_c, O_c	$V_AO_5(O_bH)$, $V_BO_5(O_cH)$, $V_CO_4(O_bH)(O_cH)$
	O_b, O_b, O_f, O_f	$V_AO_5(O_bH)$, $V_CO_4(O_bH)(O_fH)$, $V_CO_5(O_bH)$
	O_c, O_c, O_c, O_c	$V_CO_5(O_cH)$, $V_BO_4(O_cH)_2$
	O_c, O_c, O_e, O_e	$V_AO_5(O_eH)$, $V_BO_4(O_cH)(O_eH)$, $V_CO_5(O_cH)$
6†	O_b, O_b, O_c, O_c, O_e, O_e	$V_AO_2(O_bH)_2(O_eH)_2$, $V_BO_5(O_eH)$, $V_BO_4(O_cH)_2$, $V_CO_5(O_eH)$, $V_CO_4(O_cH)(O_eH)$

† The assignment of the protonated sites in this case has been made arbitrarily.

The variety of protonation states available (from 0 to 6) and types of oxo ligands (seven different types, Table 2, 3 and Fig. 1)) and vanadium atoms (three types, Fig. 1) results in a large number of possibilities, preventing a full analysis of the effect of protonation of different oxygen sites on the local geometry of the VO_6 groups. However, some common features of the protonation events have been found among the 83 structures of V_{10} with different protonation states (Table 2). The most common motifs that were submitted to a shape analysis are: $V_AO_5(O_bH)$, $V_BO_5(O_cH)$, $V_CO_5(O_bH)$, $V_CO_5(O_cH)$ and $V_CO_4(O_bH)(O_cH)$, Table 3. The results for the cases where Ob and Oc are protonated are shown in Fig. 5, where the distribution of the octahedral shape measures of those vanadium centers are compared to those of the corresponding unprotonated VO_6 groups. Fig. 5 shows that only in the case of V_C does the protonation of the O_b site promote a significant additional distortion of the coordination

octahedral. The fact that a significant change is observed for the V_C site is to be expected because it contains a V=O. However, at this position little change was observed with the normalized polyhedral when comparing deprotonated and protonated structural data, Fig. 4. Even the protonation of the O_f site that converts an oxo into a hydroxo group does not have a significant effect on the angular arrangement of the V_C-O bonds, except for a bond distance elongation, Fig. 5. This observation is remarkable, because in general the V_{10} / V_9Mo anions are viewed as pretty inflexible and in such case one would have anticipated that significant effects on the angular arrangement would have resulted. However, comparison of the structural parameters of different V_{10} anions show that the system is actually pretty flexible, because for example the protonation will be countered by changes on the other side of the cluster. That is the overall structure is distorted but maintaining its overall structure. As a result these structural changes observed upon replacement of a V-atom appear to be much more fluid and gradual and thus can explain the lack of response upon any change observed for V_A and V_B.

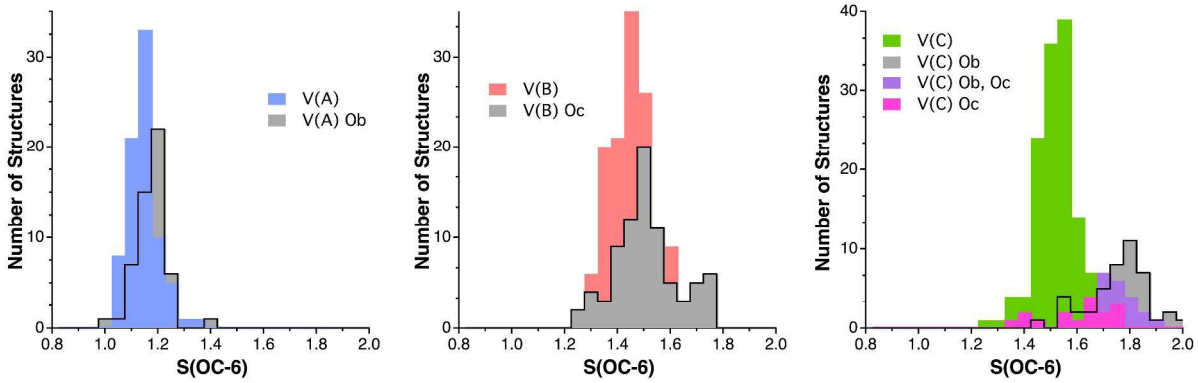

Fig. 5. Comparison of the distribution of the octahedral shape measures (S(OC-6)) for the unprotonated V_A (blue bins), V_B (red bins) and V_C (green bins) centers with those of the most common protonated centers (grey, purple and pink bins).

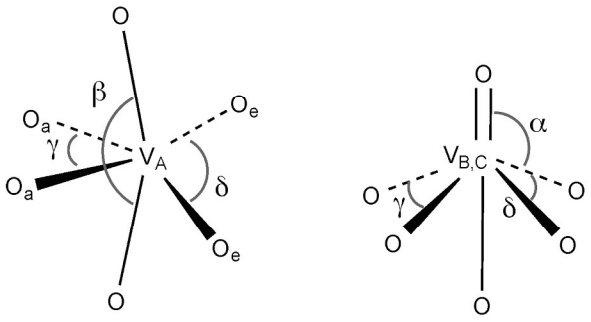

	V_{10}		PtV_9
	V_A	Pt_A	V_A
β	156 (8)	168.4	151.6
γ	78.1 (4)	85.3	76.2
δ	107 (7)	98.7	108.6
	V_B	V_C	V_C (O_bH)
α	102.0 (4)	101.3 (3)	101.5 (4)
β	174 (1)	174 (1)	172 (2)
γ	82.9 (9)	76.1 (8)	74.1 (9)
δ	92.1 (9)	95 (1)	96 (10)

Table 3. Average geometric parameters for the V_A, V_B and V_C atoms in bare decavanadate structures in the CSD (standard deviation in parentheses), in V_C with O_b protonated, and for the Pt_A and V_A atoms in PtV_9.

The occupation of different regions of the shape map by the three types of V atoms in V_{10} indicate different distortions for each of them, schematically shown in Table 3 together with averages of the relevant bond angles. The V_A atom presents a significant bending of the two axial O_b atoms, together with a strong asymmetry of the equatorial bond angles. The V_B and V_C atoms, on the other side, present a practically linear O=V-O fragment and a strong pyramidalization towards the doubly bonded oxygen atom (O_g and O_f, respectively), and a

significantly higher asymmetry in the equatorial bond angles in V_C than in V_B. The shift of the octahedral shape measures of the V_C atoms upon protonation of their O_b ligands (Fig. 5c) seems to reflect relatively small variations (of about 2°) in the bond angles, according to the data in Table 3.

Finally, we analyze the effect of substituting a Pt for a V atom on the geometries of the coordination polyhedra in V_{10} as a representative sample for a polyoxometalate with a heteroatom in the lattice, Fig. 1c. The Pt atom is larger than the Mo-atom, but the placement of the Pt in the cluster replacing the center V-atoms is likely to be less disruptive in the shape of the molecule. The CShM analysis allows us to assess the distortions and Fig. 6 plots the shape measures for the PtV_9 compound in a shape map together with the V_{10} atoms. The results revealing how drastic changes occur in the metal coordination spheres, particularly in the Pt and V centers at the V_A sites, Fig. 6a. The PtO_6 core is much closer to a perfect octahedron than the V atoms in the V_A site in V_{10}, and this results in substantially more distortion for the remaining V_A atom compared to the parent V_{10} atoms. The other V atoms in neighboring positions to Pt (two V_B and four V_C atoms) present also different coordination geometries than in the V_{10} anion, Fig. 6b and 6c. The two V_B atoms adjacent to V_A essentially retain the shape they have in the unsubstituted V_{10}. That is, the Pt atom in PtV_9 has a coordination geometry much closer to the octahedron, and the V atom at the other V_A position, is more severely distorted than in the bare or protonated V_{10} anions.

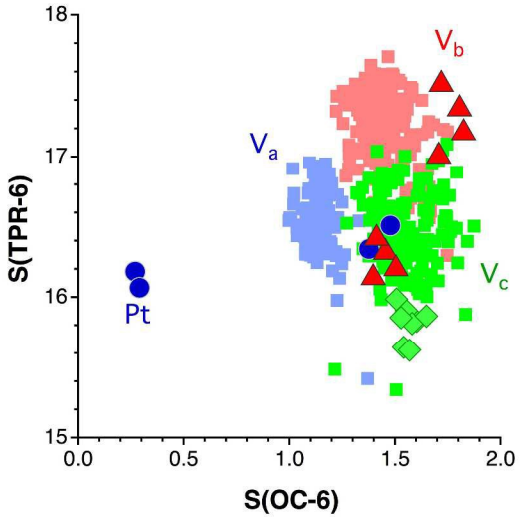

Fig. 6. Position of the MO_6 octahedra of the $H_2PtV_9O_{28}^{5-}$ anion in an octahedron-trigonal prism shape map. Circles (blue) correspond to the Pt and V_A centers, triangles (red) to the V_B, and diamonds (green) to the V_C ones. The colored areas mark the position of the three types of unprotonated metals.

In summary, the studies of V_{10} and V_9Mo encapsulated by the self assembling AOT into small water droplets was carried out at pH 5.0 where the V_{10} was monoprotonated and the overall charge on the V_{10} was -5. These conditions were selected in order to have two similar oxometalates monoprotonated V_{10} and V_9Mo with the same charge. DLS size measures of POM encapsulating RMs showed insignificant differences. Because the V_{10} deprotonate in smaller AOT RMs rendering charges different, we sought other ways to explore the effect of Mo substitution into the V_{10}. We therefore considered the effect of protonation of the shapes of the V_{10} structures using CShM analysis. Because of the different types of V-atoms, some which have a V=O and others that do not, differences are anticipated, however surprisingly small difference were observed experimentally of a large oxometalate upon dissolution into a nanosized water droplet even upon changes in charges. We therefore examined the system using using CShM analysis and then subtle differences can be identified.

Perhaps the greatest surprise in this work is how little effects protonation and substitution of V-atoms in the oxometalate core have on the overall shape of the molecule. Indeed, even the deprotonation of the V_{10} in smaller AOT RMs have little impact of the size and solubilization of the oxometalate. Overall we conclude that the most important property of the oxometalate in solubilization in the AOT RM is the shape and size of the species.

V. Conclusions

This work explores the question whether a different response is observed when placing large (8.3 Å x 7.7 Å x 5.4 Å) decametalates that have different charges and polarities in a nanoscale water droplet environment of reverse micelles. Upon placement in the small AOT reverse micelles, solutions originally containing protonated HV_{10} result in spectra consistent with deprotonation of the V_{10} thus limiting the comparison of species with similar charges. The space needed for accommodation of the decavanadate and molybdenum-substituted decavanadate was also characterized. Below w_0 = 6, reverse micelles do not form, whereas they readily form containing aqueous solutions without oxometalate. These findings suggest that certain minimum hydration shell is needed to form the reverse micelles containing polyoxometalates. When the reverse micelle size precludes formation of a hydration shell around the oxometalate probe *and* hydration of the reverse micellar inner interface, the solution either phase separates or the oxometalate precipitates out from the solution.

The long axis of the V_{10} molecule along with its hydration shell fits snugly in AOT reverse micelles of w_0 = 8 and even down to w_0 = 6. In this situation the motion of decavanadate molecules is perturbed significantly as reflected in the ^{51}V NMR linewidths. In contrast to larger reverse micelles, *e.g.*, w_0 = 30, where the linewidths are very similar to those in bulk water.

Similar behavior has been observed for the structurally very similar molybdenum-substituted decavanadate. In order to determine exactly how similar the oxovanadates were structurally, we embarked on a shape measures analysis. This is the first time the shape measures method has been applied to the family of polyoxometalates. This method allowed us to determine that despite the differences in charge and polarity, the structures and shapes were very similar. We conclude that these two systems show indistinguisable hydration of both oxometalate and micellar surface groups and this was observed even though significant differences exist in charges. Combined these studies demonstrate that studies of reactions in reverse micelles will be greatly sensitive to the compounds solubilized and its location. Importantly, these polyoxometalates need hydration spheres around them and for the case of decavanadates molecular size and shape is more important than charge on oxometalate.

Acknowledgments

ISL thanks the Fulbright organization for a fellowship. Collection of the experimental data was supported by the National Science Foundation under Grant No. 0628260 (to NEL and DCC). SA thanks the Spanish *Ministerio de Economía y Competitividad*, for support through project CTQ2011-23862-C02-01.

References

1. A. Muller, A. Müller, F. Peters, M. Pope and D. Gatteschi, *Chem. Rev.*, 1998, **98**, 239.
2. A. Muller, M. Pope and A. Müller, *Angew. Chem. Int. Ed. Engl.*, 1991, **30**, 34.
3. I. A. Weinstock, *Chem. Rev.*, 1998, **98**, 113.
4. E. M. G. Barbuzzi, I. Weinstock, R. A. Heintz, M. Wemple, J. Cowan, R. Reiner, D. Sonnen, R. Heintz, J. Bond and C. Hill, *Nature*, 2001, **414**, 191.
5. Z.-M. Zhang, C. Wang, L.-S. Long and W. Lin, *J. Am. Chem. Soc.*, 2015, **137**, 3197.

6. Y. Ji, L. Huang, J. Hu, C. Streb and Y.-F. Song, *Energy Environ. Sci.*, 2015, **8**, 776.
7. R. Ma, Y. Xu and X. Zhang, *ChemSusChem*, 2015, **8**, 24.
8. A. Sap, G. Absillis and T. N. Parac-Vogt, *Dalton Trans.*, 2015, **44**, 1539.
9. S. Omwoma, C. T. Gore, Y. Ji, C. Hu and Y.-F. Song, *Coord. Chem. Rev.*, 2015, **286**, 17.
10. O. Branytska, L. J. W. Shimon and R. Neumann, *Chem. Comm.*, 2007, 3957.
11. D. Xiao Wen, P. Qing Yi, H. Yan, H. Jia Jun and W. Si Yuan, *J. Inorg. Mater.*, 2007, **22**, 369.
12. H. Li, H. Sun, W. Qi, M. Xu and L. Wu, *Angew. Chem. Int. Ed.*, 2007, **46**, 1300.
13. C. Hill, *J. Mol. Catal. A: Chem.*, 2007, **262**, 1.
14. M.-H. Chiang, J. Dzielawa, M. Dietz and M. Antonio, *J. Electroanal. Chem.*, 2004, **567**, 77.
15. C. Rocchicciolideltcheff, M. Fournier, R. Thouvenot and C. Rocchiccioli Deltcheff, *J. Chem. Soc. Faraday Trans.*, 1991, **87**, 349.
16. A. Demarco, E. Menegatti, A. De Marco, M. Enea and P. Luisi, *J. Biochem. Biophys. Methods*, 1986, **12**, 325.
17. T. K. De and A. Maitra, *Adv. Colloid Interface Sci.*, 1995, **59**, 95.
18. D. Blach, M. Pessêgo, L. García-Río, J. J. Silber, N. M. Correa and R. D. Falcone, *Langmuir*, 2014, **30**, 12130.
19. I. Piletic, H.-S. Tan and M. D. Fayer, *J. Phys. Chem. B*, 2005, **109**, 21273.
20. A.-L. Sun, F.-C. Jia, Y.-F. Zhang and X.-N. Wang, *Mikrochim. Acta*, 2015, **182**, 1169.
21. H.-S. Tan, I. Piletic and M. D. Fayer, *J. Chem. Phys.*, 2005, **122**, 174501.
22. Y. Lee, E. Cerson, C. Thangaratnarajah, P. G. Crichton, J. J. Ruprecht, M. S. King and E. R. S. Kunji, *J. Biol. Chem.*, 2015, **290**, 8206.
23. H.-S. Tan, I. Piletic, R. Riter, N. Levinger and M. D. Fayer, *Phys. Rev. Lett.*, 2005, **94**, 057405.
24. O. F. Silva, R. H. de Rossi and N. M. Correa, *RSC Advances*, 2015, **5**, 34878.
25. R. Riter, D. Willard and N. Levinger, *J. Phys. Chem. B*, 1998, **102**, 2705.
26. N. Purwanti, M. A. Neves, K. Uemura, M. Nakajima and I. Kobayashi, *Colloids Surf., B*, 2015, **466**, 66.
27. M. Amid, F. S. Murshid, M. Y. Manap and M. Hussin, *BioMed Res. Int.*, 2015, **2015**, 8.
28. G. Sando, K. Dahl and J. Owrutsky, *J. Phys. Chem. B*, 2005, **109**, 4084.
29. Y. Yang, H. Liao, Z. Tong and C. Wang, *Compos. Sci. Technol.*, 2015, **107**, 137.
30. S. Abel, F. Sterpone, S. Bandyopadhyay and M. Marchi, *J. Phys. Chem. B*, 2004, **108**, 19458.
31. S.-O. Kim, N.-J. Cho, S. R. Tabaei, J. A. Jackman and V. P. Zhdanov, *Langmuir*, 2015, **31**, 3125.
32. J. Faeder and B. M. Ladanyi, *J. Phys. Chem. B*, 2000, **104**, 1033.
33. V. R. Girardi, J. J. Silber, N. Mariano Correa and R. Darío Falcone, *Colloids Surf., A*, 2014, **457**, 354.
34. M. Hasegawa, T. Sugimura, Y. Suzaki, Y. Shindo and A. Kitahara, *J. Phys. Chem.*, 1994, **98**, 2120.
35. S. Ghosh, A. Roy, D. Banik, N. Kundu, J. Kuchlyan, A. Dhir and N. Sarkar, *Langmuir*, 2015, **31**, 2310.
36. Y. Hirose, H. Yui and T. Sawada, *J. Phys. Chem. B*, 2004, **108**, 9070.
37. J. Krishnamoorthy, S. Vivekanandan, L. D'Urso, J. Chen, C. La Rosa, A. Ramamoorthy, J. R. Brender, M. F. M. Sciacca and L. D'Urso, *J. Phys. Chem. B*, 2015, **119**, 2886.

38. I. Piletic, D. Moilanen, D. B. Spry, N. Levinger and M. D. Fayer, *J. Phys. Chem. A*, 2006, **110**, 4985.
39. A. Maitra, *J. Phys. Chem.*, 1984, **88**, 5122.
40. B. Baruah, J. Roden, M. Sedgwick, N. M. Correa, D. Crans and N. Levinger, *J. Am. Chem. Soc.*, 2006, **128**, 12758.
41. B. Baruah, D. Crans and N. Levinger, *Langmuir*, 2007, **23**, 6510.
42. D. Crans, B. Baruah and N. Levinger, *Biomed. Pharmacother.*, 2006, **60**, 174.
43. O. W. Howarth, L. Pettersson and I. Andersson, *J. Chem. Soc., Dalton Trans.*, 1989, 1915.
44. O. W. Howarth and M. Jarrold, *J. Chem. Soc., Dalton Trans.*, 1978, 503.
45. M. Aureliano and D. C. Crans, *J. Inorg. Biochem.*, 2009, **103**, 536.
46. S. Alvarez, P. Alemany, D. Casanova, J. Cirera, M. Llunell and D. Avnir, *Coord. Chem. Rev.*, 2005, **249**, 1693.
47. S. Alvarez, D. Avnir, M. Llunell and M. Pinsky, *New J. Chem.*, 2002, **26**, 996.
48. E. Corbeil and N. Levinger, *Langmuir*, 2003, **19**, 7264.
49. A. Datta, P. K. Chowdhury, K. D. Ashby and J. W. Petrich, *Photochem. Photobiol.*, 2000, **72**, 612.
50. M. A. Sedgwick, A. M. Trujillo, N. Hendricks, N. E. Levinger and D. C. Crans, *Langmuir*, 2011, **27**, 948.
51. M. Behboudnia and H. B. Bohidar, *Colloids Surf., A, Physicochemical and engineering aspects*, 2001, **178**, 313.
52. M. Zulauf and H. Eicke, *J. Phys. Chem.*, 1979, **83**, 480.
53. B. A. Andrews, D. L. Pyle and J. A. Asenjo, *Biotechnol. Bioeng.*, 1994, **43**, 1052.
54. M. G. Spirin, S. B. Brichkin and V. F. Razumov, *Zh. Nauch. Prikl. Fotog.*, 2000, **45**, 20.
55. D. Crans and P. Shin, *Inorg. Chem.*, 1988, **27**, 1797.
56. D. Crans, C. Rithner and L. Theisen, *J. Am. Chem. Soc.*, 1990, **112**, 2901.
57. M. Pinsky and D. Avnir, *Inorg. Chem.*, 1998, **37**, 5575.
58. M. Llunell, D. Casanova, J. Cirera, P. Alemany and S. Alvarez, *SHAPE*, Version 1.21, Barcelona, 2003.
59. F. H. Allen, *Acta Crystallogr., Sect. B: Struct. Crystallogr. Cryst. Chem.*, 2002, **58**, 380.
60. A. Belsky, M. Hellenbrandt, V. Karen and P. Luksch, *Acta Crystallogr., Sect. B: Struct. Sci.*, 2002, **58**, 364.
61. N. Samart, J. Saeger, K. J. Haller, M. Aureliano and D. C. Crans, *J. Mol. Eng. Mat.*, 2014, **2**, 1440007.
62. B. Baruah, L. Swafford, D. Crans and N. Levinger, *J. Phys. Chem. B*, 2008, **112**, 10158.
63. D. Crans and N. Levinger, *Acc. Chem. Res.*, 2012, **45**, 1637.
64. I. Piletic, D. Moilanen, N. Levinger and M. D. Fayer, *J. Am. Chem. Soc.*, 2006, **128**, 10366.
65. N. Hunt, A. Jaye and S. Meech, *Chem. Phys. Lett.*, 2005, **416**, 89.
66. J. J. Silber, A. Biasutti, E. Abuin and E. Lissi, *Adv. Colloid Interface Sci.*, 1999, **82**, 189.
67. A. Chatkon, P. B. Chatterjee, M. A. Sedgwick, K. J. Haller and D. C. Crans, *Eur. J. Inorg. Chem.*, 2013, **2013**, 1859.
68. X. P. Zhan, *Chin. J. Inorg. Chem.*, 2003, **19**, 831.
69. H.-C. Joo, K.-M. Park and U. Lee, *Acta Crystallogr. Sect. E*, 2011, **67**, m1801.
70. U. Lee, H.-C. Joo, K.-M. Park, S. Mal, U. Kortz, B. Keita and L. Nadjo, *Angew. Chem. Int. Ed.*, 2008, **47**, 793.

71. S. Konaka, Y. Ozawa and A. Yagasaki, *Inorg. Chem. Commun.*, 2008, **11**, 1267.
72. S. Konaka, Y. Ozawa, T. Shonaka, S. Watanabe and A. Yagasaki, *Inorg. Chem.*, 2011, **50**, 6183.
73. A. Fukui, Y. Ozawa and A. Yagasaki, *Polyhedron*, 2012, **42**, 149.
74. A. G. Swallow, F. R. Ahmed and W. H. Barnes, *Acta Crystallogr.*, 1966, **21**, 397.
75. A. Durif, M. T. Averbuch-Pouchot and J. C. Guitel, *Acta Crystallogr. B*, 1980, **36**, 680.
76. P. Roman, A. Aranzabe, A. Luque and J. M. Guttierrez-Zorilla, *Mater. Res. Bull.*, 1991, **26**, 731.
77. A. Iida and T. Ozeki, *Acta Crystallogr. C*, 2004, **60**, i43.
78. R. Ksiksi, M. Graia, A. Driss and T. Jouini, *Acta Crystallogr. E: Struct. Rep. Online*, 2004, **60**, i105.
79. J. M. Nieto, P. Salagre, F. Medina and J. E. Sueiras, *Acta Crystallogr. C*, 1993, **49**, 1879.
80. R. K. Rastsvetaeva, *Kristallografiya*, 1999, **44**, 1027.
81. J. M. Hughes, M. Schindler and C. A. Francis, *Can. Mineral.*, 2005, **43**, 1379.
82. G. A. Bogdanovic, N. Bosnjakovic-Pavlovic, A. Spasojevic-de Bire, N. E. Ghermani and U. Mioc, *Journal of Serb. Chem. Soc.*, 2007, **72**, 545.
83. A. R. Kampf and I. M. Steele, *Can. Mineral.*, 2008, **46**, 679.
84. A.-L. Xie and C.-A. Ma, *Acta Crystallogr. C*, 2005, **61**, i67.
85. L. Uk, *Acta Crystallogr. E: Struct. Rep. Online*, 2006, **62**, i176.
86. G. Hongxu and Y. Zhongliang, *Acta Crystallogr. C*, 2007, **63**, i51.
87. J. Nilsson, E. Nordlander, U. Behrens and D. Rehder, *Acta Crystallogr. E:, Struct. Rep. Online*, 2010, **66**, i30.
88. U. Lee and H.-C. Joo, *Acta Crystallogr. E:, Struct. Rep. Online*, 2003, **59**, i122.
89. L. Y. Kang and F. Y. Long, *Chin. J. Chem.*, 2010, **28**, 2404.
90. G. Maciejewska, M. Nosek, T. Glovyak, J. Starosta and M. Cieslak-Golonka, *Polyhedron*, 2003, **22**, 1415.
91. K.J.Haller, A. Chatkon, A.Barres, N.Samart and D.C.Crans, *Inorg.Chim. Acta*, 2014, **420**, 85.
92. I.Sanchez-Lombardo, E.Sanchez-Lara, A.Perez-Benitez, A. Mendoza, S.Bernes and E.Gonzalez-Vergara, *Eur.J.Inorg.Chem.*, 2014, 4581.
93. M.Pavliuk, V.G.Makhankova, O.V.Khavryuchenko, V.N.Kokozay, I.V.Omelchenko, O.V.Shishkin and J.Jezierska, *Polyhedron*, 2014, **81**, 597.
94. H. Pang, X. Meng, H. Ma, B. Liu and S. Li, *Z.Naturforsch.,B:Chem.Sci.*, 2012, **67**, 855.
95. A.S.Rao, T.Arumuganathan, V.Shivaiah and S.K.Das, *J.Chem.Sci.(Bangalore,India)*, 2011, **123**, 229.
96. M.Jiang, Y.-T.Han, Y.-T.Li, Z.-Y.Wu and C.-W.Yan, *Pol.J.Chem.*, 2009, **83**, 1849.
97. Y. Gong, C. Hu, H. Li, W. Tang, K. Huang and W. Hou, *J.Mol.Struct.*, 2006, **784**, 228.
98. C. Yuan, L. Lu, M. Zhu, Q. Ma and Y. Wu, *Acta Crystallogr.,Sect.E:Struct.Rep.Online*, 2009, **65**, m267.
99. S.Pacigova, E.Rakovsky, M.Sivak and Z.Zak, *Acta Crystallogr.,Sect.C:Cryst.Struct.Commun.*, 2007, **63**, m419.
100. S.Yerra, S.Supriya and S.K.Das, *Inorg.Chem.Commun.*, 2013, **35**, 54.
101. F.Yraola, F.Albericio, M.Royo and X.Solans, *Z.Kristallogr.-New Cryst.Struct.*, 2008, **223**, 45.
102. E.Rakovsky, D.Joniakova, R.Gyepes, P.Schwendt and Z.Micka, *Cryst.Res.Technol.*, 2005, **40**, 719.

103. H.Kumagai, M.Arishima, S.Kitagawa, K.Ymada, S.Kawata and S.Kaizaki, *Inorg.Chem.*, 2002, **41**, 1989.
104. C.-L. Wang, J. Fu, H. Mei, D.-W. Yan and Y. Xu, *Wuji Huaxue Xuebao(Chin.)(Chin.J.Inorg.Chem.)*, 2012, **28**, 176.
105. S.-X. Liu, H.-J. Zhai, J. Peng, D.-H. Li, Z.-M. Dai, E.-B. Wang, N.-H. Hu and H.-Q. Jia, *Gaodeng Xuexiao Huaxue Xuebao(Chin.)(Chem.J.Chin.Univ.(Chinese Edition))*, 2004, **25**, 997.
106. C.-Y. Zhu, Y.-T. Li, J.-D. Wu, Z.-Y. Wu and X. Wu, *Acta Crystallogr.,Sect.E:Struct.Rep.Online*, 2007, **63**, m1777.
107. X. Wang, H.-X. Liu, X.-X. Xu and X.-Z. You, *Polyhedron*, 1993, **12**, 77.
108. I.Correia, F.Avecilla, S.Marcao and J.C.Pessoa, *Inorg.Chim.Acta*, 2004, **357**, 4476.
109. E.Rakovsky and R.Gyepes, *Acta Crystallogr.,Sect.E:Struct.Rep.Online*, 2006, **62**, m2108.
110. W. Xu, F. Jiang, Y. Zhou, K. Xiong, L. Chen, M. Yang, R. Feng and M. Hong, *Dalton Trans.*, 2012, **41**, 7737.
111. L.Jouffret, M.Rivenet and F.Abraham, *Inorg.Chem.Commun.*, 2010, **13**, 5.
112. H. Liu, J. Wang and Y. L. F. Jian, *J.Chem.Cryst.*, 2011, **41**, 1254.
113. Y. Yang, L. Xu, F. Li and X. Qu, *Inorg.Chem.Commun.*, 2013, **33**, 142.
114. R. F. d. Luis, M.K.Urtiaga, J.L.Mesa and M.I.Arriortua, *Acta Crystallogr.,Sect.E:Struct.Rep.Online*, 2010, **66**, m323.
115. J. Yan, H. Zhao, Z. Li, Y. Xing, X. Zeng, M. Ge and S. Niu, *J.Cluster Sci.*, 2009, **20**, 717.
116. S. Wang, L. Lu, S. Feng and M. Zhu, *Acta Crystallogr.,Sect.E:Struct.Rep.Online*, 2010, **66**, m632.
117. A.S.J.Wery, J.M.Gutierrez-Zorrila, A.Luque, P.Roman and M.Martinez-Ripoll, *Polyhedron*, 1996, **15**, 4555.
118. G.Asgedom, A.Sreedhara, J.Kivikoski and C.P.Rao, *Polyhedron*, 1997, **16**, 643.
119. T.McGlone, J.Thiel, C.Streb, D.-L. Long and L.Cronin, *Chem.Commun.*, 2012, **48**, 359.
120. W. Hou, J. Guo, Z. Wang and Y. Xu, *J.Coord.Chem.*, 2013, **66**, 2434.
121. P.Y.Zavalij, T.Chirayil, M.S.Whittingham, V.K.Pecharsky and R.A.Jacobson, *Acta Crystallogr.,Sect.C:Cryst.Struct.Commun.*, 1997, **53**, 170.
122. S. Lin, Q. Wu, H. Tan and E. Wang, *J.Coord.Chem.*, 2011, **64**, 3661.
123. A.Ramanan and K.Pavani, *Private Communication*, 2004.
124. L. Chen, Z.-Z. Lin, F.-L. Jiang, D.-Q. Yuan and M.-C. Hong, *Jiegou Huaxue(Chin.J.Struct.Chem.)*, 2005, **24**, 1186.
125. J. Yang, K. Huang, Z. Pu, Y. Gong, H. Li and C. Hu, *J.Mol.Struct.*, 2006, **789**, 162.
126. F.Yraola, S.Garcia-Vicente, L.Marti, F.Albericio, A.Zorzano and M.Royo, *Chem.Biol.Drug.Des.*, 2007, **69**, 423.
127. L.Klistincova, E.Rakovsky and P.Schwendt, *Transition Met.Chem.*, 2010, **35**, 229.
128. M.I.Khan, S.Tabussum and C. Zheng, *Synth.React.Inorg.Met.-Org.Chem.*, 2000, **30**, 1773.
129. Y.-T. Li, C.-Y. Zhu, Z.-Y. Wu, M. Jiang and C.-W. Yan, *Transition Met.Chem.*, 2010, **35**, 597.
130. Q.-H. Zhao, L. Du and R.-B. Fang, *Acta Crystallogr.,Sect.E:Struct.Rep.Online*, 2006, **62**, m360.
131. D.C.Crans, M.Mahroof-Tahir, O.P.Anderson and M.M.Miller, *Inorg.Chem.*, 1994, **33**, 5586.
132. M.T.Averbuch-Pouchot, *Z.Kristallogr.*, 1995, **210**, 371.

133. S.-Y.Luo, X.-L.Wu, Q.-P.Hu, J.-X.Wang, C.-Z.Liu and Y.-Y.Sun, *Zh.Strukt.Khim.(Russ.)(J.Struct.Chem.)*, 2012, **53**, 935.
134. C.Ninclaus, D.Riou and G.Ferey, *Acta Crystallogr.,Sect.C:Cryst.Struct.Commun.*, 1996, **52**, 512.
135. Y.-T. Li, C.-Y. Zhu, Z.-Y. Wu, M. Jiang and C.-W. Yan, *Transition Met.Chem.*, 2010, **35**, 597.
136. H. Zhai, S. Liu, J. Peng, N. Hu and H. Jia, *J.Chem.Cryst.*, 2004, **34**, 541.
137. E.Rakovsky, L.Zurkova and J.Marek, *Cryst.Res.Technol.*, 2001, **36**, 339.
138. J.M.Arrieta, A.Arnaiz, L.Lorente, C.Santiago and G.Germain, *Acta Crystallogr.,Sect.C:Cryst.Struct.Commun.*, 1988, **44**, 1004.
139. Z. Yi, X. Yu, W. Xia, L. Zhao, C. Yang, Q. Chen, X. Wang, X. Xu and X. Zhang, *CrystEngComm*, 2010, **12**, 242.
140. S. Meicheng, Z. Zeying, B. Chunan, Z. Lin and T. Youqi, *Zhongguo Kexue,B Ji:Huaxue(Chin.)(Sci.China,Ser.B)*, 1985, 775.
141. M.Kondo, K.Fujimoto, T.Okubo, A.Asami, S.Noro, S.Kitagawa, T.Ishii and H.Matsuzaka, *Chem.Lett.*, 1999, 291.
142. E.Rakovsky and R.Gyepes, *Acta Crystallogr.,Sect.E:Struct.Rep.Online*, 2006, **62**, m1820.
143. J.-X. Lin, J. Lu, R. Cao, J.-T. Chen and C.-Y. Su, *Dalton Trans.*, 2009, 1101.
144. M.Graia, R.Ksiksi and A.Driss, *Acta Crystallogr.,Sect.E:Struct.Rep.Online*, 2009, **65**, m953.
145. Y.-K. Lv, Z.-G. Jiang, L.-H. Gan, M.-X. Liu and Y.-L. Feng, *CrystEngComm*, 2012, **14**, 314.
146. S.-X. Liu, H.-J. Zhai, J. Peng, D.-H. Li, Z.-M. Dai, E.-B. Wang, N.-H. Hu and H.-Q. Jia, *Gaodeng Xuexiao Huaxue Xuebao(Chin.)(Chem.J.Chin.Univ.(Chinese Edition))*, 2004, **25**, 997.
147. N.C.Kasuga, M.Umeda, H.Kidokoro, K.Ueda, K.Hattori and K.Yamaguchi, *Cryst.Growth Des.*, 2009, **9**, 1494.
148. B.Yotnoi, S.Yimklan, T.J.Prior and A.Rujiwatra, *J.Inorg.Organomet.Polym.Mater.*, 2009, **19**, 306.
149. C.Santiago, A.Arnaiz, L.Lorente, J.M.Arrieta and G.Germain, *Acta Crystallogr.,Sect.C:Cryst.Struct.Commun.*, 1988, **44**, 239.
150. M. Yu, H.-j. Zai and S.-x. Liu, *Fenzi Kexue Xuebao(Chin.)(J.Mol.Sci.)*, 2006, **22**, 67.
151. D.Rehder and D. Wang, *Private Communication*, 2003.
152. A.Dewan, D.K.Kakati and B.K.Das, *Indian J.Chem.,Sect.A:Inorg.,Bio-inorg.,Phys.,Theor.Anal.Chem.*, 2010, **49**, 39.
153. I.Correia, F.Avecilla, S.Marcao and J.C.Pessoa, *Inorg.Chim.Acta*, 2004, **357**, 4476.
154. A.Sarkar and S.Pal, *Polyhedron*, 2008, **27**, 3472.
155. S. W. Ng, *Acta Crystallogr.,Sect.E:Struct.Rep.Online*, 2011, **67**, m811.
156. E.Rakovsky and L.Krivosudsky, *Acta Crystallogr.,Sect.E:Struct.Rep.Online*, 2014, **70**, m225.
157. M.Shahid, P.K.Sharma, Anjuli, S.Chibber and Z.A.Siddiqi, *J.Cluster Sci.*, 2014, **25**, 1435.
158. S.Nakamura and T.Ozeki, *Dalton Trans.*, 2008, 6135.
159. L.Klistincova, E.Rakovsky, P.Schwendt, G.Plesch and R.Gyepes, *Inorg.Chem.Commun.*, 2010, **13**, 1275.

160. A.E.Lapshin, Yu.I.Smolin, Yu.F.Shepelev, L.Zhurkova and D.Depesheva, *Kristallografiya(Russ.)(Crystallogr.Rep.)*, 1997, **42**, 677.
161. M.Farahbakhsh, P.Kogerler, H.Schmidt and D.Rehder, *Inorg.Chem.Commun.*, 1998, **1**, 111.
162. K.Pavani, S.Upreti and A.Ramanan, *J.Chem.Sci.(Bangalore,India)*, 2006, **118**, 159.
163. M.Schulz-Dobrick and M.Jansen, *Inorg.Chem.*, 2007, **46**, 4380.
164. H. Ma, X. Meng, J. Sha, H. Pang and L. Wu, *Solid State Sci.*, 2011, **13**, 850.
165. S.S.Mal, O.Troppner, I.Ivanovic-Burmazovic and P.Burger, *Eur.J.Inorg.Chem.*, 2013, 1960.
166. E.Kioseoglou, C.Gabriel, S.Petanidis, V.Psycharis, C.P.Raptopoulou, A.Terzis and A.Salifoglou, *Z.Anorg.Allg.Chem.*, 2013, **639**, 1407.
167. S.Nakamura and T.Ozeki, *J.Chem.Soc.,Dalton Trans.*, 2001, 472.
168. E.Chinea, D.Dakternieks, A.Duthie, C.A.Ghilardi, P.Gili, A.Mederos, S.Midollini and A.Orlandini, *Inorg.Chim.Acta*, 2000, **298**, 172.
169. N.-H.Hu, T.Tokuno and K.Aoki, *Inorg.Chim.Acta*, 1999, **295**, 71.
170. A.S.J.Wery, J.M.Gutierrez-Zorrila, A.Luque, P.Roman and M.Martinez-Ripoll, *Polyhedron*, 1996, **15**, 4555.
171. L. Chen, C.-Y. Yue, D.-Q. Yuan, F.-L. Jiang and M.-C. Hong, *Acta Crystallogr.,Sect.E:Struct.Rep.Online*, 2007, **63**, m675.
172. N.Strukan, M.Cindric and B.Kamenar, *Polyhedron*, 1997, **16**, 629.
173. M.Farahbakhsh, H.Schmidt and D.Rehder, *Chem.Ber.*, 1997, **130**, 1123.
174. B.Pecquenard, P.Y.Zavalij and M.S.Whittingham, *Acta Crystallogr.,Sect.C:Cryst.Struct.Commun.*, 1998, **54**, 1833.
175. Z.A.Siddiqi, Anjuli, P.K.Sharma, M.Shahid, Md.Khalid, A.Siddique and S.Kumar, *J.Mol.Struct.*, 2012, **1029**, 86.
176. W. Hou, J. Guo, Z. Wang and Y. Xu, *J.Coord.Chem.*, 2013, **66**, 2434.
177. T.Duraisamy, N.Ojha, A.Ramanan and J.J.Vittal, *Chem.Mater.*, 1999, **11**, 2339.
178. D.Riou, O.Roubeau and G.Ferey, *Z.Anorg.Allg.Chem.*, 1998, **624**, 1021.
179. T.Ito, M.Taira, K.Fukumoto, K.Yamamoto, H.Naruke and K.Tomita, *Bull.Chem.Soc.Jpn.*, 2012, **85**, 1222.
180. S.Yerra, B.K.Tripuramallu and S.K.Das, *Polyhedron*, 2014, **81**, 147.
181. I.Khan, S.Ayesh, E.Yohannes and R.J.Doedens, *Front.Biosci.*, 2003, **8**, a177.
182. E.Rakovsky, L.Zurkova and J.Marek, *Monatsh.Chem.*, 2002, **133**, 277.
183. P.Roman, A.Aranzabe, A.Luque, J.M.Gutierrez-Zorilla and M.Martinez-Ripoll, *J.Chem.Soc.,Dalton Trans.*, 1995, 2225.
184. W. Wang, F.-L. Zeng, X. Wang and M.-Y. Tan, *Polyhedron*, 1996, **15**, 265.

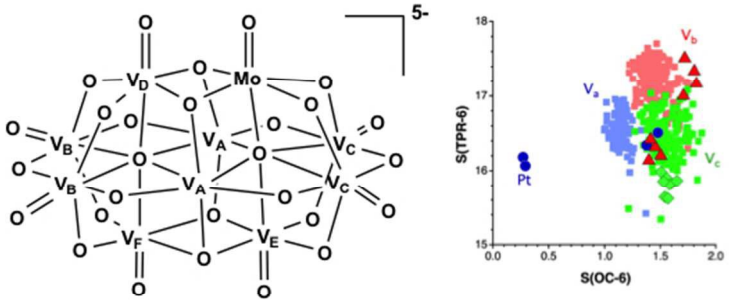

254x190mm (72 x 72 DPI)

Using ^{51}V NMR spectroscopy, dynamic light scattering and continuous shape analysis to characterize encapsulation of two polyoxometalate in reverse micelles.